Baltic Astronomy, vol. 17, 67–77, 2008

RUPRECHT 1: A SMALL, MODERATELY YOUNG OPEN CLUSTER IN THE THIRD GALACTIC QUADRANT

A. E. Piatti[1], J. J. Clariá[2], M. C. Parisi[2] and A. V. Ahumada[2]

[1] *Instituto de Astronomía y Física del Espacio, CC 67, Suc. 28, 1428 Ciudad de Buenos Aires, Argentina*

[2] *Observatorio Astronómico, Universidad Nacional de Córdoba, Laprida 854, 5000 Córdoba, Argentina*

Received 2008 February 21; accepted 2008 April 10

Abstract. We present CCD observations in the *Washington* system C and T_1 passbands down to $T_1 \sim 18.5$ in the field of Ruprecht 1, a poorly studied open cluster located in the third Galactic quadrant. We measured T_1 magnitudes and $C - T_1$ colors for a total of 862 stars distributed throughout an area of $13.6' \times 13.6'$. The cluster turned out to be very small; its linear radius being 2.6 ± 0.2 pc, as estimated from star counts in appropriate-sized boxes distributed throughout the entire field observed. By fitting the zero-age main sequence to the T_1 vs. $C - T_1$ color-magnitude diagram, we derive $E_{B-V} = 0.25 \pm 0.05$, independently from the cluster's metallicity. Our analysis suggests that Ruprecht 1 is moderately young. In fact, adopting the theoretical metal contents $Z = 0.02$ and 0.008, which provide the best global fits, we derive heliocentric distances of $d = 1.9 \pm 0.4$ kpc and 1.5 ± 0.3 kpc and ages of 200 ± 47 Myr and 251 ± 58 Myr in each case.

Key words: open clusters: individual (Ruprecht 1) – open clusters: general – techniques: photometric: Washington system

1. INTRODUCTION

As it is well known, Galactic open clusters cover a large range of distances, ages and metallicities (Friel 1995; Friel et al. 2002). This characteristic justifies their use in investigations of the chemical and dynamical evolution of our Galaxy. Such investigations, however, require high-quality data about the greatest possible number of open clusters.

The present work is part of a current project of photometric observation in the *Washington* system of some unstudied or poorly studied Galactic open clusters. Our goal is to determine their basic parameters or to refine the quality of their observationally determined properties. We have already reported results based on *Washington* CCD photometric observations on the relatively young open clusters NGC 2194 and NGC 2324 (Piatti et al. 2003a, 2004b), intermediate-age clusters NGC 2627 and Tombaugh 1 (Piatti et al. 2003b, 2004c), old metal-poor anticenter cluster Trumpler 5 (Piatti et al. 2004a) and the moderately metal-poor Hyades-like age NGC 2236 (Clariá et al. 2007).

The present paper is devoted to Ruprecht 1, a small-sized open cluster in the Canis Major constellation. This cluster is located at J2000: $\alpha = 6^{\rm h}36^{\rm m}25^{\rm s}$, $\delta =$

$-14^\circ\,10'\,48''$ and $\ell = 223.99^\circ$, $b = -9.69^\circ$. Both Ruprecht (1966) and Archinal & Hynes (2003) classified it as belonging to class III3p, i.e., a poor open cluster composed of bright and faint stars, without any noticeable concentration. Lyngå (1987) reported $3'$ as an angular radius of the cluster. A catalogue of 2.5 million stars with proper motions in the *Hipparcos* system and B, V magnitudes in the Johnson photometric system has been compiled by Kharchenko (2001). Their resulting All-Sky Compiled Catalogue (ASCC-2.5) can be retrieved from the CDS[1]. More recently, Kharchenko et al. (2005, hereafter KPRSS) presented a catalogue of astrophysical data for 520 Galactic open clusters – among them Ruprecht 1 – which could be identified in their ASCC-2.5. By applying homogeneous methods and algorithms, KPRSS determined angular sizes and basic parameters for their cluster sample. For Ruprecht 1, they estimated an angular radius of $15'$ and obtained the following results: $E_{B-V} = 0.15$, $d = 1100$ pc and age 575 Myr. It should be noted, however, that due to the relatively bright limiting magnitude ($V \approx 12.5$) of the ASCC-2.5, KPRSS's sample does not include faint and generally remote or highly obscured open clusters. According to KPRSS, their cluster sample is sufficiently complete for clusters up to 1 kpc.

In the present study in the field of Ruprecht 1 we report the results obtained from CCD photometry in the C and T_1 passbands of the *Washington* system up to $T_1 \approx 18.5$. These data are used to make a new and independent determination of reddening, distance, age and metallicity. In Section 2 we present the observational material and the data reduction. In Section 3 we describe the main features of the observed color-magnitude diagram (CMD) and determine the cluster center and stellar density radial profile. In Section 4, by fitting theoretical isochrones computed for the *Washington* system we determine basic parameters of the cluster. Finally, a brief summary of our main conclusions is presented in Section 5.

2. OBSERVATIONS AND REDUCTIONS

CCD images of the cluster field were obtained with the 0.9 m telescope at Cerro Tololo Inter-American Observatory (CTIO, Chile) during the night of 2004 December 19–20. The telescope was equipped with a CCD camera with the 2048×2048 pixel Tektronix 2K No. 3 chip with a pixel size of 24 μm which yielded a scale of $0.4''$ per pixel (focal ratio f/13.5) and a field of $13.6' \times 13.6'$. The *Washington* C and the Kron-Cousins $R_{\rm KC}$ filters were used. These filters were recommended by Geisler (1996) who has shown that the $R_{\rm KC}$ filter has significant advantages over the standard *Washington* T_1 filter. Since both filters have similar transmittances, hereafter we will use the designation T_1, usual for the *Washington* system. The CCD camera was controlled through the CTIO ARCON 3.3 data acquisition system in the standard quad amplifier mode, operating at a mean measured gain (four chips) of 2.00 ± 0.04 e$^-$ ADU^{-1}, with a mean readout noise of 3.60 ± 0.15 e$^-$. Under photometric sky conditions (the typical seeing was $1.1''$) we obtained two 150 s exposures for the C band, and two 10 s exposures for the $R_{\rm KC}$ band, with a mean air mass of 1.13. At the beginning of the observing night, we obtained a series of 10 bias and 5 dome and sky flat-field exposures per filter. In order to standardize our photometry, images of 34 standard stars from the lists of Landolt (1992) and Geisler (1996), covering a wide color range, were obtained. In particular, stars in the area PG 0231+051 were observed at low and high air masses in

[1] ftp://cdsarc.u-strasbg.fr/pub/cats/I/280A

order to adjust the extinction coefficients properly.

We reduced the CCD images at the Instituto de Astronomía y Física del Espacio (Argentina) with IRAF[2] using the QUADPROC package. We applied bias subtraction to all the images and flat-fielding to both standard and program field images, employing weighted combined signal-calibrator frames. The resulting processed images turned out to be satisfactorily flat. We then derived the instrumental magnitudes for the standard stars from aperture photometry using DAOPHOT/IRAF routines (Stetson et al. 1990). We obtained the following transformation equations between instrumental and standard magnitudes through least square fits:

$$c = (3.727 \pm 0.023) + T_1 + (C - T_1) + (0.271 \pm 0.010) \times X_C - (0.080 \pm 0.009) \times (C - T_1), \quad (1)$$

$$r = (3.272 \pm 0.008) + T_1 + (0.089 \pm 0.004) \times X_{T_1} - (0.028 \pm 0.003) \times (C - T_1), \quad (2)$$

where X represents the effective air mass, and capital and lowercase letters stand for standard and instrumental magnitudes, respectively. The coefficients were derived through the IRAF routine FITPARAM, resulting in rms errors of 0.022 for c and 0.009 for r. The instrumental magnitudes for stars in the Ruprecht 1 field were obtained from point-spread function (PSF) fits using stand-alone versions of the DAOPHOT[3] and ALLSTAR[3] programs, which provided us with x and y coordinates and instrumental c and r magnitudes for all stars identified in each field.

For each frame, a quadratically varying PSF was derived by fitting ~ 100 stars, once the neighbors were eliminated by using a preliminary PSF. The preliminary PSF was obtained from 35-40 brightest, least contaminated stars. Both groups of PSF stars were interactively selected. We then used the ALLSTAR program to apply the resulting PSF to the identified stellar objects and to create a subtracted image, which was used to find and measure magnitudes of additional fainter stars. The PSF magnitudes were determined using the aperture magnitudes yielded by the task PHOT as zero points. This procedure was repeated three times for each frame. Finally, we computed aperture corrections from the comparison of PSF and aperture magnitudes using the subtracted neighbor PSF star sample. The resulting aperture corrections were -0.01 and 0.00 mag for c and r images, respectively.

Next, we separately combined all the measures for the c, r exposure pairs using the stand-alone DAOMATCH[3] and DAOMASTER[3] programs. We thus obtained two tables which list the running number of stars, the x and y coordinates, the c and r magnitudes, and the respective observational errors for each measured star. The standard magnitudes and colors for all the measured stars were computed through equations (1) and (2), excluding stars having only c or r magnitudes. Once we obtained the standard magnitudes and colors, we finally built a master table containing the average magnitudes T_1 and color indices $C - T_1$, their

[2]IRAF is distributed by the National Optical Astronomy Observatories, which is operated by the Association of Universities for Research in Astronomy, Inc., under contract with the National Science Foundation

[3]Program kindly provided by P.B. Stetson

errors $\sigma(T_1)$ and $\sigma(C-T_1)$ (or the observational ones if only one measure of T_1 and $C-T_1$ was available), and the number of observations. Table 1 provides the magnitudes and colors for a total of 862 stars measured in the field of Ruprecht 1. Only a fragment of this table is presented here as an example. The complete table is available upon request from the first author.

Table 1. Results of CCD photometry in the C, T_1 system for stars in the field of Ruprecht 1.

Star	x (pixel)	y (pixel)	T_1 (mag)	$\sigma(T_1)$ (mag)	$C-T_1$ (mag)	$\sigma(C-T_1)$ (mag)	n
33	1035.509	127.264	15.127	0.040	2.633	0.061	2
34	1178.344	140.434	17.816	0.028	1.895	0.039	2
35	812.357	142.701	17.490	0.038	1.686	0.002	2
...	...	...	...	...	...	...	...
...	...	...	...	...	...	...	...

NOTE: (x,y) coordinates correspond to the reference system of Figure 3.

3. COLOR-MAGNITUDE DIAGRAM FEATURES

Figure 1 shows the T_1 vs. $C-T_1$ CMD for all the observed stars in the field of Ruprecht 1. Note that the cluster main sequence can be more easily identified at $T_1 < 15$ since the contamination by field stars increases for fainter stars.

To estimate the input of background stars in the lower part of the main sequence, we started by determining the location of the cluster center and plotting the cluster star density profile. This straightforward approach allows us not only to adopt an optimum cluster radius, but also to obtain the CMD dominated by cluster stars. However, some field star contamination is unavoidable.

We fitted Gaussian distributions to the star counts in the x and y directions of the field, approximately parallel to the directions of right ascension and declination, to determine the coordinates of the cluster center and to estimate their uncertainty. The numbers of stars projected along the x and y directions were counted within the intervals 50 pixels wide, although we checked that using bins from 25 to 50 pixels or from 50 to 100 pixels does not change significantly the derived center. The selected size of the box allowed us to sample statistically the star spatial distribution and to avoid spurious effects mainly caused by the presence of localized groups, rows or columns of stars. The fit of a single Gaussian was performed using the NGAUSSFIT routine in the STSDAS/IRAF package. The center of the Gaussian, its amplitude and its full width at half-maximum (FWHM) acted as variables, while the constant and the linear terms were fixed to the value of the background level (the density of field stars was assumed to be uniform) and to zero, respectively. After eliminating a couple of discrepant points, a significant improvement in the fitting procedure was achieved. The cluster center was finally determined with a typical standard deviation of ± 10 pixels ($\sim 4''$).

Then we constructed the cluster radial profile by computing the number of stars per unit area at a given radius r with the formula:

$$(n_{r+25} - n_{r-25})/((m_{r+25} - m_{r-25}) \times 50^2), \tag{3}$$

where n_j and m_j represent the number of stars and boxes included in a circle of

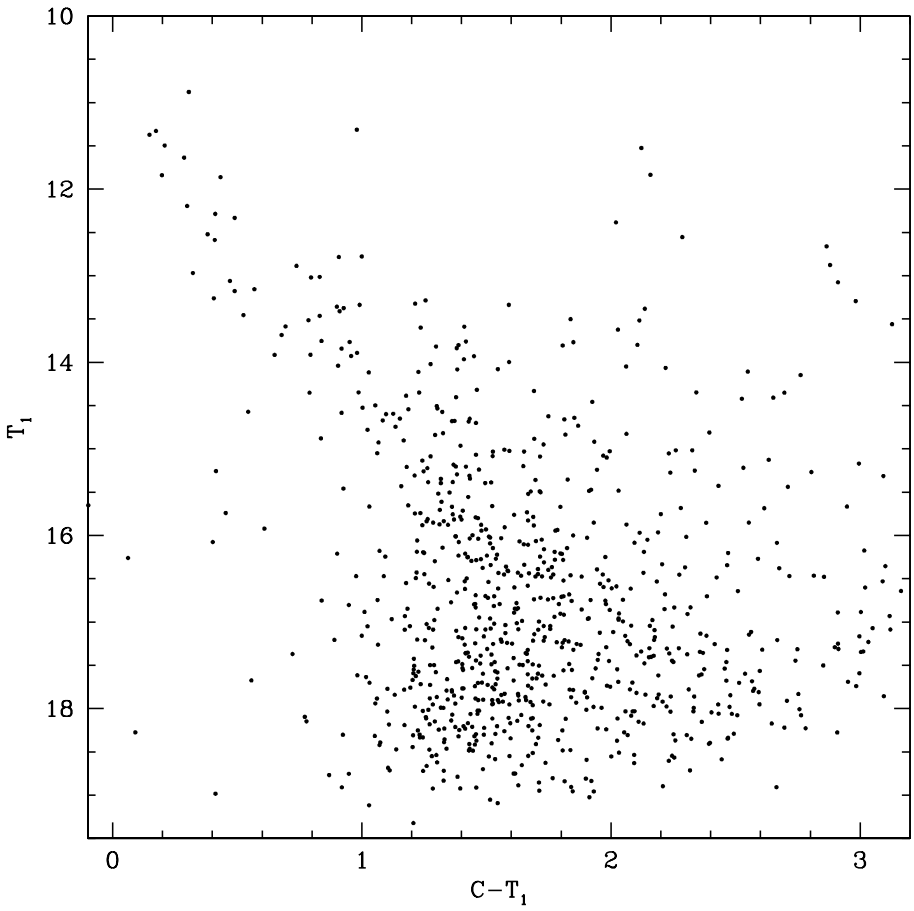

Fig. 1. T_1 vs. $C - T_1$ CMD for stars observed in the field of Ruprecht 1.

radius j, respectively. Note that this expression easily allows one to estimate the mean star density at the radius r without the need of tracing a complete circle at that distance in the observed field. This is an important consideration in the sense that we have a stellar density profile which extends far away from the cluster center. This allows us to estimate the background level with higher precision. Since we define the cluster radius as the distance from the cluster center where the number of stars per unit area equals that of the background, it follows that the more precise the background level, the more exact cluster radius is estimated. On the other hand, it is also helpful to measure the FWHM of the stellar density profile and to determine the variation (in percentage) of the field star contamination in relation to the distance from the cluster's center. In this way, we have a reference to perform circular extractions including mostly the cluster star population and to build reliably a purified CMD of the cluster.

The resulting density profile expressed as a number of stars per unit area in pixels is shown in Figure 2. It corresponds to the region around the cluster center up to 1200 pixels. The background region of Ruprecht 1 was delimited by the ob-

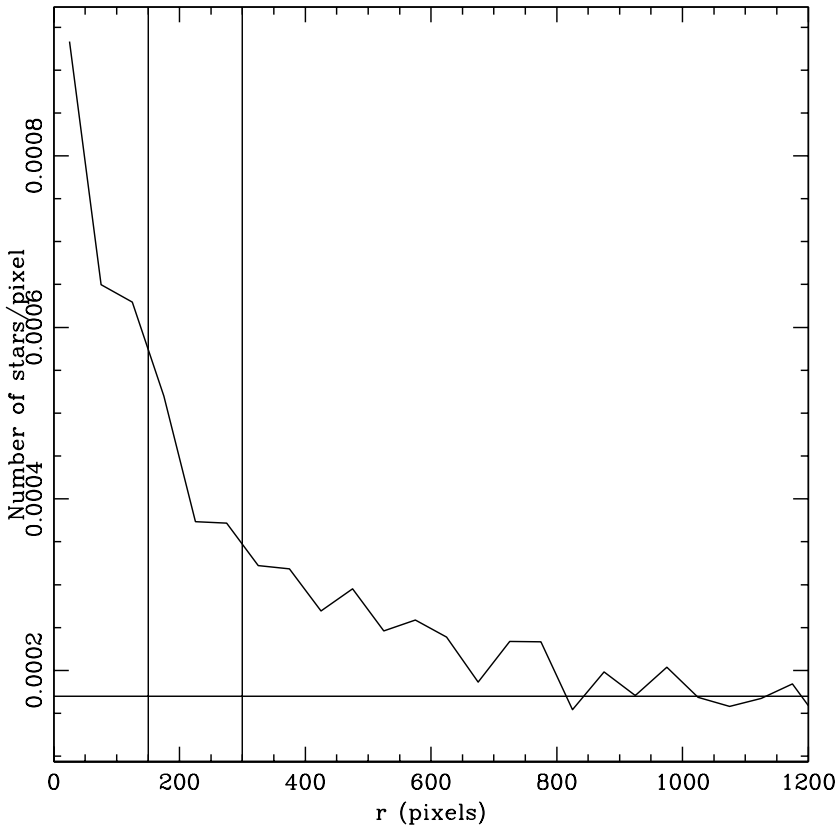

Fig. 2. Star density radial profile centered on Ruprecht 1. The horizontal line represents the measured background level, while the vertical lines correspond to $r_{\rm FWHM}$ and $r_{\rm clean}$ (see Section 3 for details).

served field boundaries and by a circle of 900 pixel radius from the center. The calculated background level resulted in $(17 \pm 2) \times 10^{-5}$ stars/pixels, which leads to an estimated cluster radius of $r_{\rm cls} = 800 \pm 50$ pixels, equivalent to an angular radius of $5.3' \pm 0.4'$. This value is somewhat larger than the $3.0'$ given by Lyngå(1987) but is considerably smaller than $15'$, the value given by Kharchenko et al. (2005). The cluster angular radius derived here compares well with the $4.8'$ given by Kharchenko et al. for the cluster core radius. The radius at the FWHM ($r_{\rm FWHM}$) and the estimated radius which maximizes the star cluster population and minimizes the field star contamination in the CMD ($r_{\rm clean}$) was found to be 150 and 300 pixels, respectively. We finally derived the field star contamination of 22 %, 38 % and 68 % for the radial intervals $r < r_{\rm FWHM}$, $r_{\rm FWHM} < r < r_{\rm clean}$ and $r_{\rm clean} < r < r_{\rm cls}$, respectively. Note that the percentage of field stars is relatively low in the central region and even for $r < r_{\rm clean}$, while no cluster stars are clearly seen in the surrounding field between $r_{\rm clean}$ and $r_{\rm cls}$.

Figure 3 shows three CMDs constructed including different circular extractions around the cluster. We also show the schematic finding chart of Ruprecht 1 in the left top panel of the figure. The sizes of symbols are proportional to the T_1 bright-

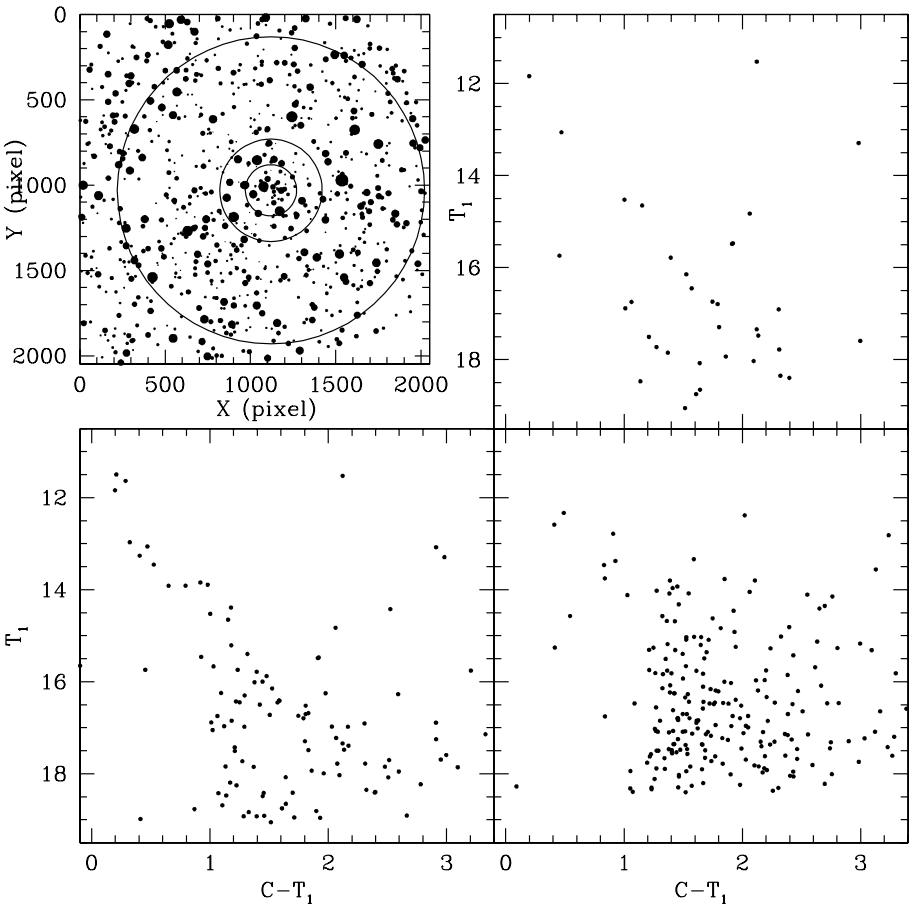

Fig. 3. Upper left panel: schematic finding chart of the stars observed in the field of Ruprecht 1. The three concentric circles correspond to the extracted CMDs for: $r < r_{\rm FWHM}$ (upper right panel), $r < r_{\rm clean}$ (bottom left panel), and $r > r_{\rm field}$ (bottom right panel). North is up and east is to the left.

ness of stars. The panels in the figure exhibit the variations of star population from the innermost to the outermost regions of the cluster field. We start with the CMD for stars distributed within r $r < r_{\rm FWHM}$, followed by CMD for the cluster regions delimited by $r < r_{\rm clean}$ and finally by the adopted field CMD. We used the CMD corresponding to the stars within $r_{\rm FWHM}$ as the cluster fiducial sequence reference. Then, we performed different circular extractions by varying the distance from the cluster center, in order to build an optimum cluster CMD. This results from a compromise between maximizing the number of cluster stars and minimizing the field star contamination. Finally, we chose that CMD which exhibits the best enhanced cluster fiducial features (left bottom panel of Figure 3). The associated distance to this CMD is called $r_{\rm clean}$.

What first attracts our attention is the fact that the cluster main sequence (MS) does not show clear signs of evolution except for three turnoff stars and a probable red giant star located at $T_1 \approx 11.5$. The remarkable feature is the length

of the MS covering ~ 6 magnitudes. These features are hints that we are dealing with a relatively young open cluster. The width of the MS does not appear to be due to photometric errors, since these hardly reach a tenth of magnitude at any T_1 level. Notice that the field stars also have magnitude and color distribution which is different from that of the cluster's MS. This is seen if we compare the right (field) with the left (cluster) bottom panels in Figure 3. In the subsequent analysis, we will use the CMD with $r < r_{\rm clean}$ for the cluster.

4. BASIC PARAMETERS OF THE CLUSTER

To estimate the reddening, distance, age and metallicity of Ruprecht 1 we applied theoretical isochrones computed recently for the *Washington* photometric system (Lejeune & Schaerer 2001; Girardi et al. 2002). We prefer the latter isochrones calculated with the core overshooting effect which reach fainter magnitudes, allowing a better fit to the cluster's MS. We initially decided to use metallicities $Z = 0.02$ and 0.008 for the isochrone sets varying in steps of $\Delta \log t = 0.05$ dex.

First, we fitted the zero-age main sequence (ZAMS) to the T_1 vs. $C - T_1$ diagram and derived the color excess E_{C-T_1} and the apparent distance modulus $T_1 - M_{T_1}$ for each selected metallicity. The relatively long cluster's MS allowed to determine these parameters accurately. By using $E_{C-T_1}/E_{B-V} = 1.97$ and $A_{T_1}/E_{B-V} = 2.62$ (Geisler et al. 1996), we derive $(E_{B-V},\ V - M_V) = (0.25 \pm 0.05,\ 12.25 \pm 0.25)$ and $(0.25 \pm 0.05,\ 11.75 \pm 0.25)$ for $Z = 0.02$ and 0.008, respectively. Therefore, the cluster appears to be more reddened than previously believed.

Next, we selected isochrones of some hundred million years of age, younger than the Hyades, and used the two derived pairs of $(E_{B-V},\ V - M_V)$ values to estimate the cluster age. In order to reach an adjustment which best resembles the cluster features, we assumed different scenarios: (i) the three brightest MS stars observed in the cluster CMD are considered to be the top of the sequence; (ii) the red star located at $(C - T_1,\ T_1) \approx (2.1,\ 11.5)$ is considered to be a red giant clump star of the cluster; (iii) both hypotheses are combined. We did not find any isochrone which would fit reasonably the assumed top of the MS, its entire length and the red giant clump locus. This happens for the both adopted metallicities.

Finally, we fitted the observed cluster MS without any assumption about the brightest turnoff magnitude of the cluster. The isochrones which most properly reproduce the cluster features in the $C-T_1$ vs. T_1 diagram proved to be those with $\log t = 8.3 \pm 0.1$ and 8.4 ± 0.1 for $Z = 0.02$ and 0.008, respectively. In either case, the cluster is younger than previously considered. To match these isochrones, we used the E_{C-T_1} color excesses and the $T_1 - M_{T_1}$ apparent distance moduli derived for each metallicity independently. The uncertainties of these ages were estimated from the dispersion of the cluster features. Figure 4 shows the best fits of the ZAMS and the isochrones for $Z = 0.02$ and 0.008. Note that both sets of adjusted isochrones are not distinguishable within the errors. The largest difference is observed at the start of the core helium burning phase, where no stars are seen. Thus, we cannot favor any of the two assumed Z values for the cluster until the additional information will be received. It would be important to know whether the star at $(C - T_1, T_1) = (2.1,\ 11.5)$ is a cluster spectroscopic binary or a field giant.

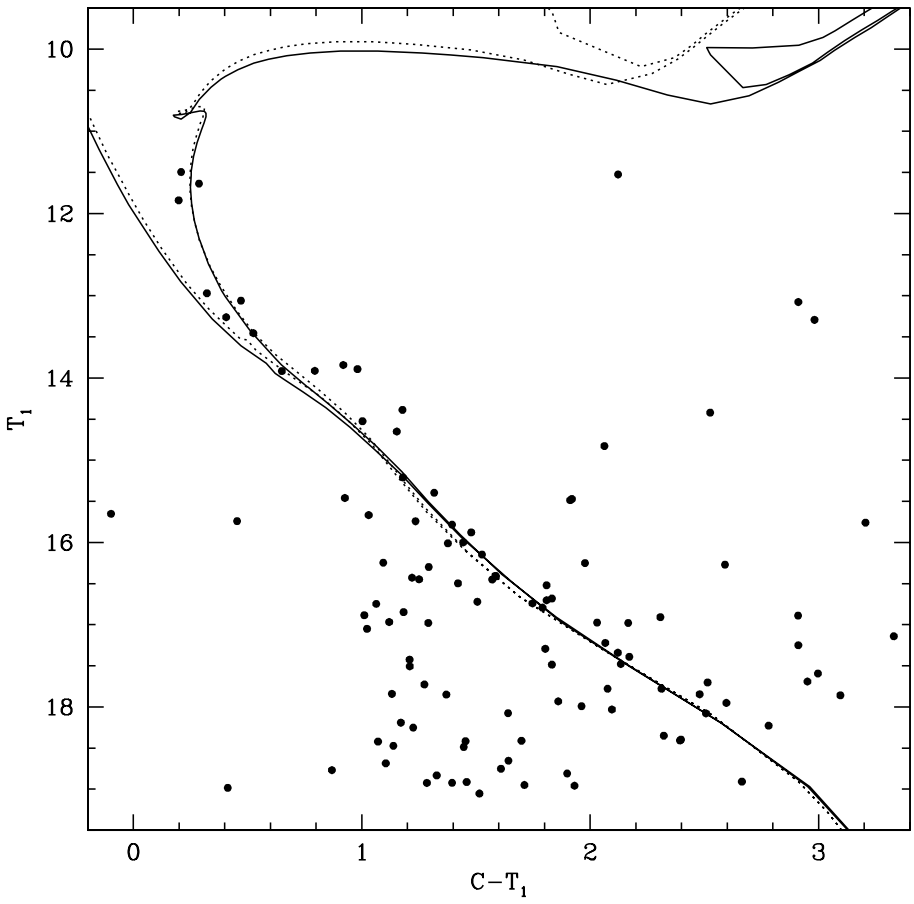

Fig. 4. The CMD for stars within $r < r_{\rm clean}$. The ZAMS lines and the isochrones are from Girardi et al. (2002) for Z = 0.02 and 0.008 (solid and dotted lines, respectively.

From the derived cluster reddenings and apparent distance moduli, we obtained its distances from the Sun, $d = 1.9 \pm 0.4$ kpc and 1.5 ± 0.3 kpc, for Z = 0.02 and 0.008 respectively. The distance errors were derived bearing in mind the expression $0.46\times[\sigma(V-M_V) + 3.2\times\sigma(E_{B-V})]\times d$, where $\sigma(V-M_V)$ and $\sigma(E_{B-V})$ represent the estimated errors in $V-M_V$ and E_{B-V} respectively. An average value of 1.7 kpc for the cluster distance from the Sun yields (9.706, –1.164, –0.286) kpc for the Galactic coordinates (X, Y, Z). If we assume the galactocentric distance of the Sun $R_{GC} = 8.5$, the galactocentric distance for Ruprecht 1 is $R_{GC} = 9.79$ kpc. The linear of the cluster 2.6 ± 0.2 pc, i.e., it is quite small. Our value is little more than 1/3 of the tidal radius recently estimated by Piskunov et al. (2008).

5. CONCLUDING REMARKS

In this paper we present CCD photometry in the C and T_1 filters of the *Washington* system for 862 stars in the field of the southern open cluster Ruprecht 1. The results have been used to plot a T_1 vs. $C - T_1$ CMD reaching down to

$T_1 \sim 18.5$. Ruprecht 1 is found to be a very small, moderately young open cluster. The analysis of the present photometric data leads to the following main conclusions.

(i) The observed T_1 vs. $C - T_1$ CMD reveals a relatively long cluster main sequence (MS) extending ~ 6 magnitudes. The width of the MS is mainly caused by intrinsic features, such as binarity and/or evolutionary effects, although a number of field stars, particularly at $T_1 > 15$, are also present.

(ii) Fitting the ZAMS to the T_1 vs. $C - T_1$ CMD and using $E_{C-T_1}/E_{B-V} = 1.97$, we derive $E_{B-V} = 0.25 \pm 0.05$, a value that is considerably larger than 0.15 derived by Kharchenko et al. (2005). With the present E_{B-V} we find that the cluster sequences are best reproduced by isochrones $\log t = 8.3$ and 8.4 for $Z = 0.02$ and 0.008, respectively. However, some evidence exists that the cluster might be of solar metallicity. Heliocentric distances $d = 1.9 \pm 0.4$ kpc and 1.5 ± 0.3 kpc are determined for $Z = 0.02$ and 0.008 respectively. Consequently, the cluster is found to be younger and located farther from the Sun than it was considered before.

(iii) The radius of the cluster, $5.3' \pm 0.4'$, corresponding to 2.6 ± 0.2 pc, was estimated from star counts within and outside the cluster area. The current angular radius is significantly smaller than the value of $15'$ given by Kharchenko et al. (2005).

ACKNOWLEDGMENTS. We are gratefully indebted to the CTIO staff for their hospitality and support during the observing run. The present work was partially supported by the Argentinian institutions CONICET and SECYT (Universidad Nacional de Córdoba). This work is based on observations made at Cerro Tololo Inter-American Observatory, which is operated by AURA, Inc., under cooperative agreement with the National Science Foundation.

REFERENCES

Archinal B. A., Hynes S. J. 2003, *Star Clusters*, Willman-Bell, Inc.
Clariá J. J., Piatti A. E., Parisi M. C., Ahumada A. V. 2007, MNRAS, 379, 159
Drimmel R., Spergel D. N. 2001, ApJ, 556, 181
Friel E. D. 1995, ARA&A, 33, 382
Friel E. D., Janes K. A., Tavarez M., Scott J., Katsanis R., Lotz J., Hong L., Natham M. 2002, AJ, 124, 2693
Geisler D. 1996, AJ, 111, 480
Geisler D., Clariá J. J., Minniti D. 1991, AJ, 102, 1836
Geisler D., Lee M. G., Kim E. 1996, AJ, 111, 1529
Girardi L., Bertelli G., Bressan A., Chiosi C., Groenewegen M. A. T. et al. 2002, A&A, 391, 195
Kharchenko N. V. 2001, Kinematic and Physics of Celestial Bodies, 17, 409
Kharchenko N. V., Piskunov A. E., R"oser S., Schilbach E., Scholz R.-D. 2005, A&A, 438, 1163
Landolt A. 1992, AJ, 104, 340
Lyngå G. 1987, *Catalogue of Open Cluster Data*, CDS, Strasbourg
Lejeune T., Schaerer D. 2001, A&A, 366, 538
Mermilliod J.-C., Paunzen E. 2003, A&A, 410, 511
Piatti A. E., Clariá J. J., Abadi M. G. 1995, AJ, 110, 2813

Piatti A. E., Clariá J. J., Ahumada A. V. 2003a, MNRAS, 340, 1249
Piatti A. E., Clariá J. J., Ahumada A. V. 2003b, MNRAS, 346, 390
Piatti A. E., Clariá J. J., Ahumada A. V. 2004a, MNRAS, 418, 979
Piatti A. E., Clariá J. J., Ahumada A. V. 2004b, A&A, 421, 991
Piatti A. E., Clariá J. J., Ahumada A. V. 2004c, MNRAS, 349, 641
Piskunov A. E., Schilbach E., Kharchenko N. V., Röser S., Scholtz R.-D. 2008, A&A, 477, 172
Ruprecht J. 1966, Bull. Astron. Inst. Czech., 17, 33
Stetson P. B., Davis L. E., Crabtree D. R. 1990, in *CCDs in Astronomy*, ASP Conf. Ser., 8, 289
Tecce T. E, Pellizza L. J., Piatti A. E. 2006, Rev. Mex. A&A, Conf. Series, 26, 86